



# Flow injection amperometric detection of catechol using dual-band poly(3-methylthiophene) electrodes

Hong Zhang, Ahmed Galal, Judith F. Rubinson, Isam Marawi,  
Thomas H. Ridgway, Suzanne K. Lunsford, Hans Zimmer  
and Harry B. Mark Jr.\*

Department of Chemistry, University of Cincinnati, Cincinnati, OH 45221, U.S.A.

(Received 31 August 1997; in revised form 10 November 1997)

**Abstract**—This work reports the electrochemical detection of catechol ( $10^{-4}$  to  $10^{-6}$  M) in the presence of ascorbic acid ( $10^{-4}$  to  $10^{-6}$  M) using dual-band poly(3-methylthiophene) (P3MT) electrode flow-injection amperometry without prior separation. The selectivity involved in this method is based on the differences in electrochemical behavior of catechol and ascorbic acid. A variety of dual-band Pt, Au, glassy carbon, and P3MT electrodes were constructed and used as the electrochemical detector. The upstream electrode of the series dual-band electrode unit is used for detection of catechol and ascorbic acid and the downstream electrode for detection of the oxidized catechol. The band dimensions range from  $0.1 \times 2.5$  to  $1 \times 5.5$  mm with the interelectrode gaps varying from 0.1 to 0.5 mm. Although this method is effective for dilute solutions of catechol ( $< 10^{-5}$  M) in the presence of ascorbic acid ( $< 10^{-5}$  M) under both neutral and acidic conditions, it is not efficient for more concentrated mixtures ( $> 10^{-5}$  M) unless the measurements are made under acidic conditions such as at pH 1.6. A negative deviation from the ideal calibration curve of the oxidized catechol reduction is found in the more concentrated mixtures ( $> 10^{-5}$  M) at physiological pH 7.4. Charge-dipole interaction and hydrogen bonding between the oxidized products of catechol and ascorbic acid in the concentrated neutral solutions are proposed to explain the suppression of the current signals. Variation of the flow rates from 0.5 to 3.0 ml/min has no effect on the performance of the detector. The dual-band P3MT electrode has less positive oxidation potentials for catechol and ascorbic acid oxidation compared to the bare Pt, Au, and glassy carbon electrodes because of the catalytic activity of the P3MT electrode surface. Dual-band P3MT as well as glassy carbon electrodes have the best (highest) collection efficiency for catechol detection. The collection efficiency also remains constant when the interelectrode gaps vary from 0.1 to 0.5 mm. © 1998 Elsevier Science Ltd. All rights reserved

**Key words:** catechol, ascorbic acid, poly(3-methylthiophene), dual-band electrode for flow-injection amperometry, electrochemical reversibility.

## INTRODUCTION

Over twenty years ago, Adams reported probing brain chemistry with electroanalytical techniques [1]. In his paper, cyclic voltammetry at a graphite electrode in the brain tissue of rat detected the neurotransmitter norepinephrine and/or its metabolic precursor dopamine and also ascorbate simultaneously at 0.3 to 0.4 V versus a saturated calomel electrode. Later studies found that the major difficulty in electrochemical detection of neurotransmit-

ters ( $\sim 10^{-5}$  M) *in vivo* was the interference from excess ascorbate ( $\sim 10^{-4}$  M), which oxidized at the same potential as catecholamines. Since then, much research has concentrated on overcoming this overlapping potential problem [2]. A variety of new electrodes have been invented for the selective detection of catecholamines *in vivo*. For example, the interference from ascorbic acid in the detection of norepinephrine has been eliminated by its reaction with the enzyme ascorbic acid oxidase at an eliminator membrane for the electrode in the detection of norepinephrine [3]. Similar approaches utilized anion-repelling polymer membranes such as Nafion

\*Author to whom correspondence should be addressed.

to inhibit ascorbic acid access to the electrode [4, 5]. Catecholamines and ascorbic acid mixtures were resolved voltammetrically by incorporating stearic acid into a graphite paste electrode, which retarded electron transfer between the electrode surface and ascorbic acid [6]. Similarly, catecholamines and ascorbic acid mixtures were resolved voltammetrically as a result of large differences in the oxidation potentials for these species at poly(pyrrole) [7], poly(3-methylthiophene) (P3MT) [8], and specially treated carbon fiber electrode materials [9]. In addition, new electrochemical techniques coupled with other methods such as a modified platinum electrode used in conjunction with differential pulse voltammetry [10] and electrical stimulation in conjunction with fast cyclic voltammetry [11] have been applied for the detection of catecholamines *in vivo*. These analytical methods have been used in the direct study of neurotransmission in extracellular fluids [2, 9].

The dual working electrode technique was developed in the 1960's. Anderson and Reilley found that the limiting steady-state current was proportional to the concentration gradient of a redox couple in a thin layer of solution confined between two closely-spaced plane parallel electrodes and was inversely proportional to the interelectrode spacing [12]. Bruckenstein and coworkers were the first group to measure an intermediate collection efficiency at a rotating Pt ring-disc electrode in the electrochemical reduction of Cu(II) [13]. Dual electrochemical detectors for liquid chromatography have been widely used for the analysis of trace biological molecules such as neurotransmitters since the 1970's. The parallel or adjacent configuration of the dual electrodes was used for the identification of analytical peaks through current ratios. The series configuration, where analytes first passed the upstream electrode and then the downstream electrode, was used for selective detection [14]. For example, overlapping components of a chromatogram such as dopamine, norepinephrine, 3,4-dihydroxy-benzylamine, and 6-hydroxydopamine were separated with detection limits of  $10^{-13}$  M based on the difference of their oxidation potentials using series dual electrodes as chromatographic detectors [15, 16]. Similarly thiols and disulfides in citrus leaf homogenate and in whole blood filtrate [17], flavinoids in beer, barley, grape juice, and wines [18, 19], reversible and irreversible components in plasma, rat brain tissue homogenate, and human urine [20–23], were detected using the same method. Also the base line drift, which had been a problem for the determination of analytes with high redox potentials, could be minimized as the downstream electrode detector was set at lower potentials [24–26]. A dual electrode used for capillary electrophoresis has also been reported recently for the detection of catecholamines in the presence of ascorbic acid and phenolic acids in black tea [27].

Voltammograms of catecholamines at a carbon electrode show a quasi-reversible oxidation wave, while those of ascorbate exhibit an irreversible character because of slow electron transfer and the formation of an electroactive product [1, 9, 28]. We report here the simultaneous detection of catechol and ascorbic acid based on their differences in electrochemical behavior using series dual-band electrode flow-injection amperometry without any prior forms of separation. By applying the oxidation potential of catechol and ascorbic acid at the upstream electrode and the reduction potential of the oxidized catechol at the downstream electrode, catechol and ascorbic acid can be simultaneously detected at a dual-band electrode. The sensitivity and wide dynamic range achieved using the electroanalytical method are examined. Dual-band Pt, Au, glassy carbon, and P3MT electrodes are used as the detector for flow-injection analysis with different electrode sizes and different interelectrode gaps to evaluate their suitability in the simultaneous detection. It is interesting to study the dual-band P3MT electrode because it has the advantages of improved electrochemical reversibility, selectivity, and sensitivity for catechol detection.

## EXPERIMENTAL

### Reagents and carriers

Acetonitrile (HPLC grade), tetrabutylammonium tetrafluoroborate (TBATFB), sulfuric acid (A.C.S. Reagent), methanol (HPLC grade), and catechol, sodium phosphate, monobasic sodium phosphate, sodium chloride, all certified, were obtained from Fisher Scientific (Pittsburgh, PA). The 3-methylthiophene (3MT) monomer was obtained from Aldrich (Milwaukee, WI) and Fisher Scientific. It was stored at 4°C. Ascorbic acid (A.C.S.) and dehydroascorbic acid (A.R.) were obtained from MCB Manufacturing Chemists (Cincinnati, OH) and Aldrich, respectively. All reagents were used as received. Deionized water with 17.8 M $\Omega$ /cm resistance at room temperature was used throughout. It was obtained by purifying distilled water through a Nanopure II-apparatus (Sybron/Barnstead Company, Newton, MA).

Two electrolyte solution types were used in the FIA and CV studies. A 0.1 M phosphate + 0.1 M sodium chloride solution (pH 7.4) was made by dissolving 2.13 g of monobasic sodium phosphate, 12.26 g of sodium phosphate, and 5.84 g of sodium chloride into 1 l of deionized water. A 0.01 M sulfuric acid solution (pH 1.6) was made by diluting 0.56 ml concentrated sulfuric acid to 1 l with deionized water. All pH values were measured using a pH meter (Orion model 811, Boston, MA). The solutions were filtered using filter paper with pore size of 2  $\mu$ m (Millipore, Milford, MA) under vacuum

and then deaerated by bubbling with nitrogen for 30 min prior to flow-injection analysis.

#### Procedure for construction of the dual-band Pt, Au, and glassy carbon electrodes

Pt and Au foils, and glassy carbon plate with thickness ranging from 0.1 to 1.0 mm were obtained from Alfa/Aesar and cut to the desired dimensions. Electrical contacts to the Pt and Au pieces were made by either spot welding or soldering to copper wires. Glassy carbon electrodes were connected to copper wires using a conductive adhesive (ACME, E-SOLDER No. 3021, New Haven, CT). The dual electrode assembly was made by pressing together two electrode surfaces with a thin layer of epoxy resin (Buehler, Lake Bluff, IL). After curing, the resistance of the assembly was tested to insure that there were no short circuits between the two electrodes. The assembly was mounted vertically in the center hole of a working electrode Teflon block and sealed with epoxy resin. Excess epoxy resin was polished away from the block using 100 grit aluminum oxide sandpaper (3M, St. Paul, MN) to expose the dual-band electrode surface. A BAS standard procedure for electrode polishing [29] was followed for each electrode. The electrode unit, including Pt, Au, or glassy carbon, was roughly polished on CARBIMET Discs of grit 600 and grit 1200 (Buehler) successively using water as a lubricant. It was then polished on Nylon cloth (Buehler) using 2  $\mu\text{m}$  diamond paste (this step was not used for glassy carbon electrodes). Finally, the electrode unit was polished on Microcloth (Buehler) using 0.05  $\mu\text{m}$  alumina (Buehler). It was critical to use an individual polishing set for the different electrode materials. The freshly polished electrode unit was sonicated in methanol for 1 min, rinsed with deionized water, and dried in a stream of  $\text{N}_2$  gas. The polishing procedure was repeated until a mirror-like surface with imperfections less than micron size (as determined by optical microscopy) was achieved. Band dimensions ranged from  $0.1 \times 2.5$  for dual-band Pt and Au electrodes to  $1 \times 5.5$  mm for dual-band glassy carbon electrodes with the interelectrode gaps varying from 0.1 to 0.5 mm. The size of the interelectrode gap was determined using optical microscopy and compared to the width of the band electrode (0.1 mm).

#### Electropolymerization conditions

Electropolymerization of 3-methylthiophene at the polished dual-band electrode was carried out in a three-electrode single-compartment cell (80 ml) by applying constant potential using a PAR model 173 potentiostat/galvanostat (Princeton Applied Research, Princeton, NJ). The reference electrode was a Ag/AgCl (3 M NaCl, MF-2074, BAS, West Lafayette, IN). Its potential was checked against a

saturated calomel electrode assembly (MF-2055 and MF-2057, BAS) before repetitive use, after prolonged exposure to acetonitrile. An auxiliary electrode in the form of a coil was made from a 120 mm long, 0.3 mm diameter, Pt wire (Alfa/Aesar, Ward Hill, MA), sealed in the tip of a disposable glass pipette using epoxy. The dual-band electrode was positioned above the coil of the Pt auxiliary electrode during the electrochemical polymerization and CV studies.

Fresh monomer solution was prepared prior to each polymerization. The stock 0.05 M TBATFB/acetonitrile solution was deaerated by bubbling with argon for 10 min. After addition of the 3MT monomer, the solution was stirred and deaerated by bubbling argon for 2 min. An acetone/isopropanol bath cooled by dry ice was used for polymerization at  $-20^\circ\text{C}$ . The electropolymerization conditions were optimized to reduce growth of the P3MT polymer film beyond the electrode substrate (an edge effect relates to the fast chain propagation reaction rate of 3MT electropolymerization at a small-sized electrode and consequently increases the overall surface area of the electrode) [30]. The optimum electropolymerization conditions used for preparation of P3MT/Pt and P3MT/glassy carbon electrodes in this study are: monomer concentration 0.075 M, applied voltage 1.7 V, deposition time 10 s, temperature  $-20^\circ\text{C}$ , and TBATFB concentration 0.05 M. After the electropolymerization, the P3MT/Pt or P3MT/glassy carbon electrode was rinsed with methanol and, then, deionized water. The P3MT film thickness made under the above electropolymerization conditions was approximately 10  $\mu\text{m}$  based on optical microscopy.

#### Apparatus

A BAS-100 electrochemical analyzer (BAS) was employed for the cyclic voltammetric studies. A scan rate of 100 mV/s was used throughout the study unless otherwise stated. Optical micrographs were taken using a Nikon Optiphot microscope equipped with a Nikon model FG 35 mm camera and quartz lamp. The objective lenses of 3 $\times$  or 20 $\times$  and an ocular lens of 5 $\times$  were used. A voltmeter/ohmmeter (Fluke) was used to measure voltage and resistance.

The flow-injection analysis with an electrochemical detection system consisted of an Altex 100A double reciprocating pump (Berkeley, CA) and a Rheodyne injector (Cotati, CA) with a 20  $\mu\text{m}$  sample loop. The sample traveled through tubing with a length of 40 cm and an inner diameter of 0.5 mm. Flow rates were calculated by measuring the volume of the mobile phase that passed during a fixed time interval. The experimental error was  $\pm 5\%$ . The thin layer electrochemical cell (8  $\mu\text{l}$ ) consisted of an auxiliary electrode block with the solution inlet and outlet, a reference electrode holder,

a gasket (thickness 0.13 mm (BAS)), and a working electrode block. A series configuration dual electrode unit was used throughout this study. Constant independent dual potentials were applied using a custom built dual working electrode potentiostat, which was computer controlled [31]. The peak current with the background signal subtracted and peak time for flow-injection amperometry were automatically printed out. Data files could be saved as DFL files and converted to TXT files for further data treatment.

## RESULTS AND DISCUSSION

### Dual-band electrodes and cyclic voltammetry of catechol and ascorbic acid

Optical micrographs of a bare dual-band Au and a P3MT/Pt electrode with a band size of  $0.1 \times 2.5$  mm and an interelectrode gap of approximately 0.1 mm are shown in Fig. 1A, B. The “edge effect”, due to the P3MT film growing beyond the substrate electrode edge during the electropolymeri-

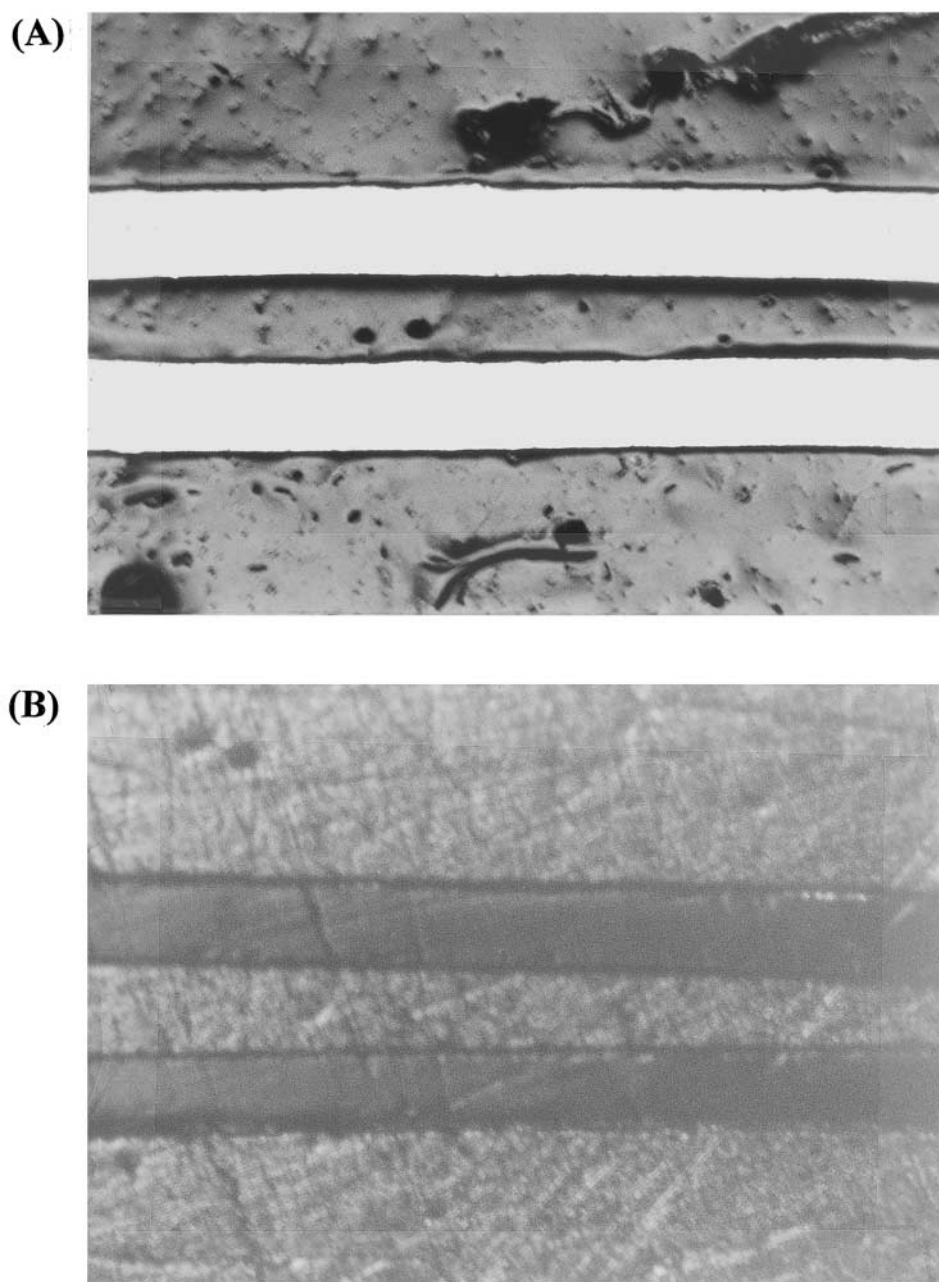


Fig. 1. Optical micrographs of dual-band electrodes: (A) Au with an interelectrode gap  $95 \mu\text{m}$  and band width  $100 \mu\text{m}$ ; (B) P3MT/Pt with an interelectrode gap  $80 \mu\text{m}$  and band width  $100 \mu\text{m}$ .

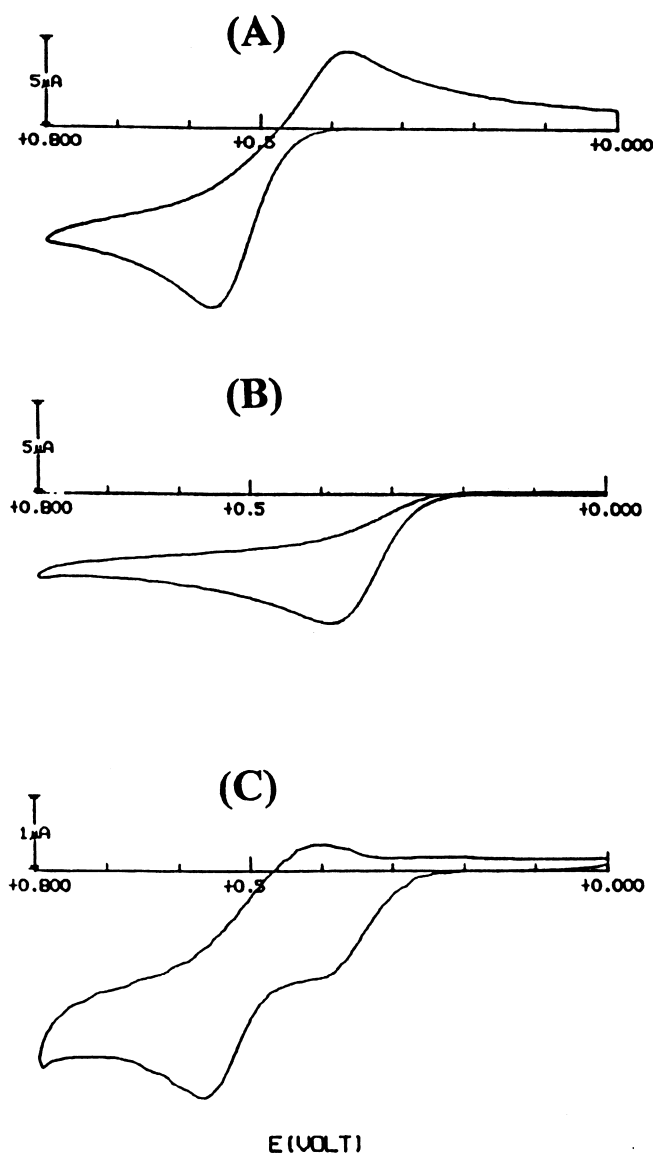


Fig. 2. Cyclic voltammograms at a P3MT/Pt electrode (inter-electrode gap  $150\ \mu\text{m}$ , band size  $2.5 \times 0.1\ \text{mm}$ ) at pH 1.6: (A) 5 mM catechol, (B) 5 mM ascorbic acid, and (C) 1 mM catechol in the presence of 1 mM ascorbic acid at a single active P3MT band electrode. Scan rate 100 mV/s; sensitivity  $1.0\text{E} - 5\ \text{A}$ ; electrolyte 0.01 M  $\text{H}_2\text{SO}_4$ .

zation, can be seen to be insignificant using the above electropolymerization conditions [30].

The selectivity principle involved in detection of catechol in the presence of ascorbic acid can be shown by the cyclic voltammograms (CV) of catechol (Fig. 2A) and ascorbic acid (Fig. 2B) at a single band of the dual-band P3MT/Pt electrode unit in the pH 1.6 solution. It is interesting to note that the P3MT film is in its neutral, non-conducting form at the potentials when the catechol CV experiments are observed. This phenomenon is not yet fully understood. It has been previously shown that the electrochemical reactions of catechol and ascorbic acid occur at or near the polymer-solution interface, and not within the polymer film [32]. The oxidation peak potentials of 5 mM catechol and

5 mM ascorbic acid are measured to be approximately 570 and 400 mV, respectively. The reduction peak potential of the oxidized catechol is about 400 mV. No reduction peak is detected for oxidized ascorbic acid as this species is electroinactive. CV's of catechol and ascorbic acid in the pH 7.4 solution at dual-band P3MT/Pt, Pt, Au and glassy carbon electrodes also show that the oxidation of catechol is reversible and that of ascorbic acid is irreversible. However, the peak potentials shift toward the more negative direction. The oxidation peak potentials for catechol are 270, 400, 330, and 440 mV for the four electrode materials at pH 7.4, respectively. The reduction peak potentials of oxidized catechol are 60, 20, 20, and  $-20\ \text{mV}$ , and the oxidation peak potentials of ascorbic acid are 210, 430, 350, and

410 mV, respectively. The CV of 1 mM catechol in the presence of 1 mM ascorbic acid (Fig. 2C) in the pH 1.6 solution at the P3MT electrode shows the resolution of the oxidation potentials of catechol at 570 mV and ascorbic acid at 400 mV, and the reduction peak of the oxidized catechol at 400 mV. In the pH 7.4 phosphate buffer solution this reduction peak is also detected at P3MT electrodes under similar experimental conditions, but the oxidation peaks of catechol and ascorbic acid are not resolved. CV's at the bare Pt electrode under similar experimental conditions at the two different pH's show that the reduction peak of the oxidized catechol is not detectable and the oxidation peaks of catechol and ascorbic acid are not resolved. Similar results were reported by Wightman and coworkers at a carbon paste electrode in a solution of  $10^{-4}$  M of dopamine in the presence of  $10^{-3}$  M of ascorbic acid at pH 7.4 [33]. These results further indicate that the reversibility of catechol oxidation is significantly improved at P3MT electrodes [8, 30].

At equal concentrations of pure catechol and ascorbic acid solutions the peak current of catechol is always larger than that of ascorbic acid (Fig. 2A, B). This current difference is observed at all electrode materials such as Pt, glassy carbon, Au, and P3MT. This could be due to either an effect of different molecular size on diffusion [34, 35] or different degree of electrocatalysis for the two species, or a combination of both. The peak current

of catechol or ascorbic acid doubles in magnitude when connecting the two bands of the dual-band electrode unit externally. Similar results are observed upon varying dual-band electrode materials and their corresponding interelectrode gaps. Thus, there is no peak current suppression due to overlapping of the diffusion layers at each band of the dual-band electrode unit. This type of suppression had been observed for closely-spaced dual ultramicroelectrodes and ultramicroelectrode arrays where the interelectrode gaps were only a few microns [36–38]. The peak current suppression led to the determination of a shielding factor,  $S$ , defined by the following equation:

$$S = 1 - T/(2Z)$$

where  $T$  is the peak current observed at the two bands connected externally, and  $Z$  is the peak current at a single active band electrode of a dual-band electrode unit. The shielding factor,  $S$ , defined above, is zero for all dual-band electrodes used in this research. This result is important for quantitative analysis at each band of the dual-band electrode unit.

#### Hydrodynamic voltammetry of catechol and ascorbic acid at dual-band electrodes

Hydrodynamic voltammograms of catechol and ascorbic acid are useful in determining the optimum potential settings for the dual-electrode in the flow-

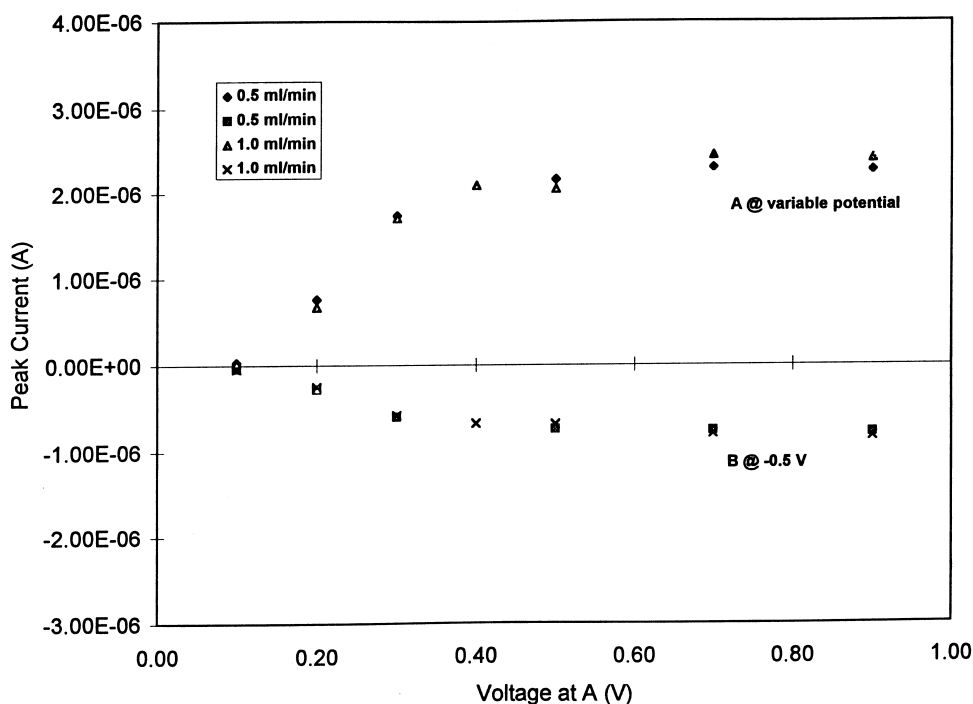


Fig. 3. Hydrodynamic voltammograms of 0.5 mM catechol at a series dual-band P3MT/Pt electrode at pH 7.4 (interelectrode gap  $150 \mu\text{m}$ , band size  $2.5 \times 0.1 \text{ mm}$ ): the potential of upstream electrode A varied as labeled; the potential of downstream electrode B fixed at  $-0.5 \text{ V}$ . Positive current stands for oxidation and negative current for reduction. Mobile phase  $0.1 \text{ M}$  phosphate buffer +  $0.1 \text{ M}$  NaCl; flow rates 0.5 and 1.0 ml/min; sensitivity  $3.6 \mu\text{A}$ .

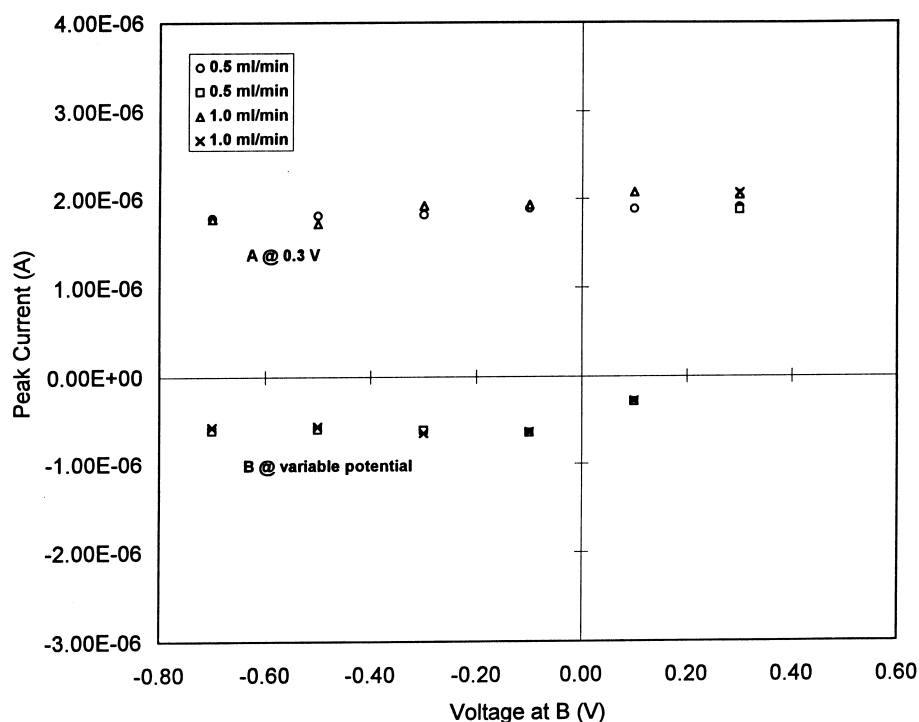


Fig. 4. Hydrodynamic voltammograms of 0.5 mM catechol at a series dual-band P3MT/Pt electrode at pH 7.4: the potential of upstream electrode A fixed at +0.3 V; the potential of downstream electrode B varied as labeled. Other experimental conditions as in Fig. 3.

injection amperometric detection. Hydrodynamic voltammograms of catechol at the upstream electrode of a dual-band P3MT/Pt electrode at pH 7.4 were constructed by varying the potential at the upstream electrode from 0 to 900 mV and fixing it at downstream electrode at -500 mV. This downstream electrode potential setting was sufficiently negative to quantitatively reduce the oxidized catechol (Fig. 3). The limiting current for catechol oxidation in the pH 7.4 solution at a P3MT/Pt dual-band electrode is reached at about 400 mV. Similar results are obtained at the upstream electrode of the bare dual-band Pt electrode for catechol oxidation, however, the limiting current is reached at more positive potential, that is, at 600 mV. For the oxidation of ascorbic acid in the pH 7.4 solution at the P3MT/Pt dual-band electrode the limiting current is reached at 400 mV. When the oxidation potential is set more positive than 400 mV, the oxidation current of catechol or ascorbic acid increases slightly. However, at potentials more positive than 400 mV the background current increases at a higher rate. In most experiments, the upstream electrode potential is set at the onset of the oxidation limiting current of catechol. For example, it is 400 mV at pH 7.4 and 600 mV at pH 1.6 for P3MT electrodes such as P3MT/Pt and P3MT/glassy carbon electrodes. This gives the most reproducible results for flow-injection analysis.

Similar comments can be made concerning the hydrodynamic voltammograms of catechol at the

downstream electrode of the dual-band P3MT/Pt electrode at pH 7.4, where the potential at the upstream electrode is fixed at 300 mV and it is varied from 300 to -700 mV at the downstream electrode (Fig. 4). The limiting current for the oxidized catechol reduction is attained at about -100 mV. The background current increases rapidly if the downstream electrode potential is set at more negative. In most experiments, the downstream electrode potential of the dual-band P3MT/Pt or P3MT/glassy carbon electrode is set at -100 mV at pH 7.4 and 100 mV at pH 1.6.

Flow rates ranging from 0.5 to 3.0 ml/min have no noticeable influence on the peak current measurements in the flow-injection amperometric detection (Figs 3 and 4) although analytes elute earlier as the flow rate increases. Residence times for the solution flow in the electrochemical cell (1 to 0.16 s) are sufficiently long for exhaustive electrolysis at the flow rate used. Other researchers have reported that FIA responses do not change at these flow rates [39].

#### Flow-injection amperometric detection of catechol in the presence of ascorbic acid using dual-band electrodes

Initially, catechol and ascorbic acid standard solutions at pH 7.4 were run individually using a dual-band P3MT/Pt electrode for the estimation of their detection limits (Figs 5 and 6). As discussed in the above section the upstream electrode potential was

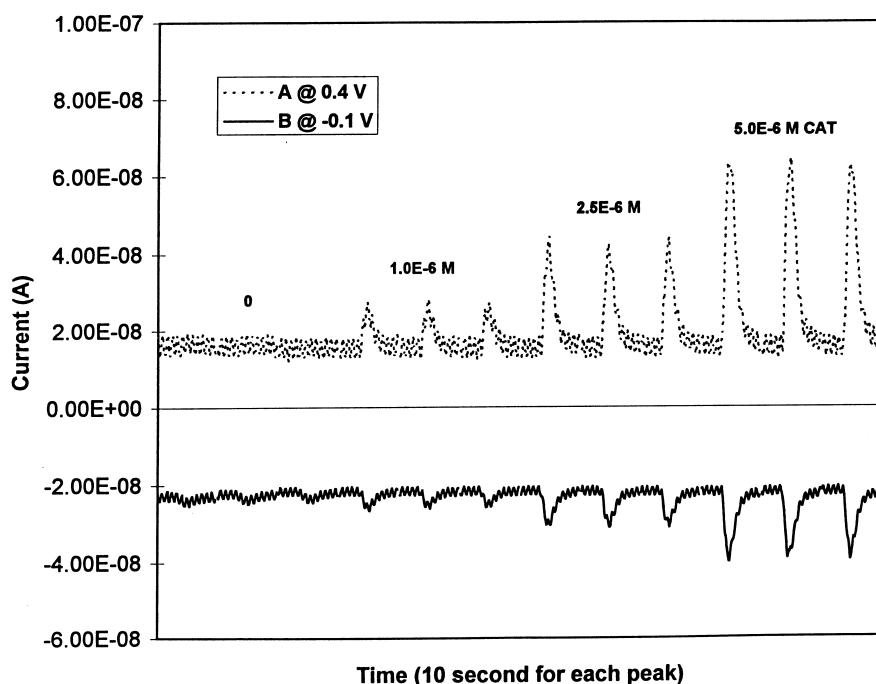


Fig. 5. Flow-injection amperometric responses of a series dual-band P3MT/Pt electrode for determination of catechol at pH 7.4 (inter-electrode gap  $150\ \mu\text{m}$ , band size  $2.5 \times 0.1\ \text{mm}$ ). Triplicate runs were made for solutions containing catechol ranging from  $1.0\text{E}-6$  to  $5.0\text{E}-6\ \text{M}$ . Potentials of the upstream A and downstream B electrodes were held at 0.4 and  $-0.1\ \text{V}$ , respectively. The positive current values are for the oxidation of catechol and the negative current values for the reduction of oxidized catechol. Mobile phase  $0.1\ \text{M}$  phosphate buffer +  $0.1\ \text{M}$  NaCl; flow rate  $1.0\ \text{ml/min}$ ; sensitivity  $90\ \text{nA}$ .

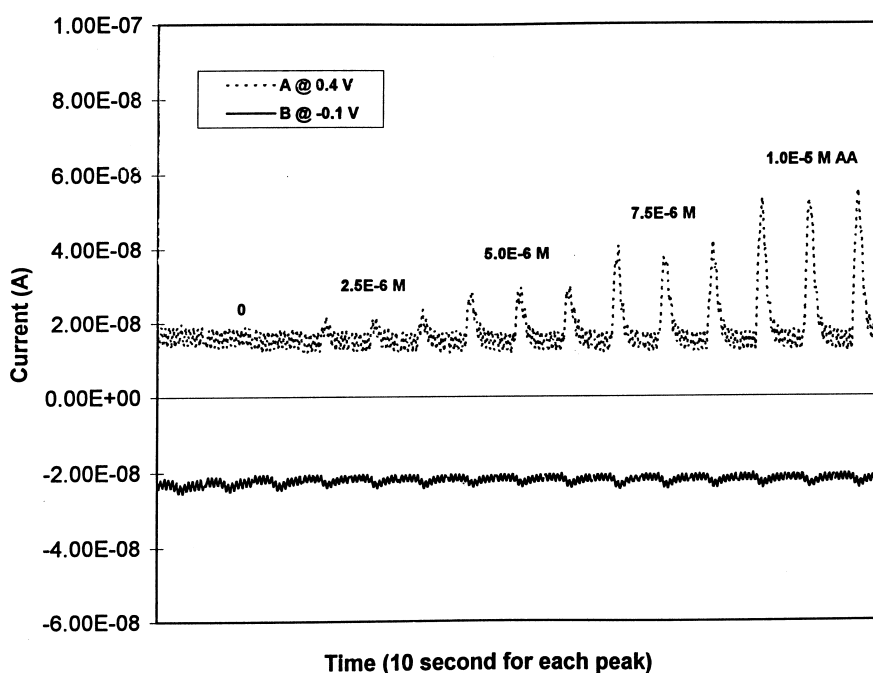


Fig. 6. Flow-injection amperometric responses of a series dual-band P3MT/Pt electrode for determination of ascorbic acid at pH 7.4. Triplicate runs were made for solutions containing ascorbic acid ranging from  $2.5\text{E}-6$  to  $1.0\text{E}-5\ \text{M}$ . Experimental conditions as in Fig. 5.

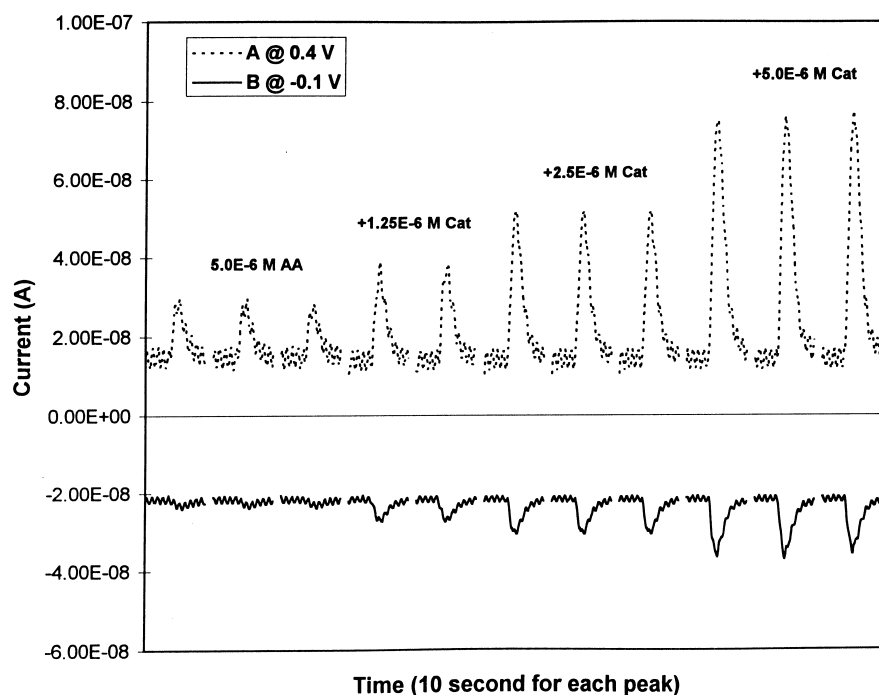


Fig. 7. Flow-injection amperometric responses of a series dual-band P3MT/Pt electrode at pH 7.4 for determination of catechol in the presence of  $5.0 \times 10^{-6}$  M ascorbic acid at pH 7.4. Triplicate runs were made for solutions containing catechol ranging from  $1.25 \times 10^{-6}$  to  $5.0 \times 10^{-6}$  M. Experimental conditions as in Fig. 5.

set at 0.4 V and the downstream electrode potential at  $-0.1$  V to achieve the limiting currents. Triplicate runs were made for each concentration. The oxidation current of catechol at the upstream electrode and the reduction current of the oxidized catechol at the downstream electrode are proportional to the catechol concentration ranging from  $1.0 \times 10^{-6}$  to  $5.0 \times 10^{-6}$  M. A detection limit is defined as a concentration of an analyte which produces a signal at least twice as high as the signal caused by the blank. Based on this definition, the detection limits for catechol at the upstream and downstream electrodes of the dual-band P3MT electrode are similar and are equal to  $1.0 \times 10^{-6}$  M. For ascorbic acid the oxidation current at the upstream electrode is also proportional to its concentration ranging from  $2.5 \times 10^{-6}$  to  $1.0 \times 10^{-5}$  M with a detection limit of  $2.5 \times 10^{-6}$  M. There is, of course, no response at the downstream electrode when the ascorbic acid concentration changes.

Catechol solutions ranging from  $1.25 \times 10^{-6}$  to  $5.0 \times 10^{-6}$  M in the presence of  $5.0 \times 10^{-6}$  M ascorbic acid were first studied to estimate the detection limit of catechol in the presence of ascorbic acid using P3MT/Pt dual-band electrode flow-injection amperometry. The molar ratios of ascorbic acid to catechol are 4:1, 2:1, and 1:1 in this study. Both oxidation and reduction currents are proportional to the catechol amount added to the  $5.0 \times 10^{-6}$  M ascorbic acid solution (Fig. 7). The detection limit for catechol in the presence of ascorbic acid, as defined previously, is therefore

$1.25 \times 10^{-6}$  M. Calibration curves for the detection of catechol, ascorbic acid, and catechol in the presence of ascorbic acid are plotted based on the above results (Fig. 8). Straight lines show that the current is proportional to the analyte concentration. The sensitivity of ascorbic acid in flow-injection analysis is less than that of catechol. This result is in agreement with the CV experiments and could also be explained by either a comparison of diffusion rates based on molecular size in the diffusion controlled electrode reaction [34, 35], or a different degree of electrocatalysis for the two species, or a combination of both. The reduction calibration line for the oxidized catechol in the presence of ascorbic acid is superimposable on that of catechol alone, while the oxidation calibration line of catechol in the presence of ascorbic acid is parallel to that of catechol alone with a positive intercept. The current value for this intercept is exactly that of a  $5.0 \times 10^{-6}$  M ascorbic acid solution. This is a very important point as it shows that in the dilute mixture solutions catechol in the presence of ascorbic acid behaves the same as its pure standard solutions. The reduction of the oxidized catechol is not interfered by the presence of ascorbic acid and its oxidized product, and the signals of catechol and ascorbic acid oxidation are additive. Therefore, the concentrations of catechol and ascorbic acid in the mixtures can be simultaneously determined based on their individual calibration plots.

The average collection efficiency for catechol is calculated by taking the ratio of the reduction cur-

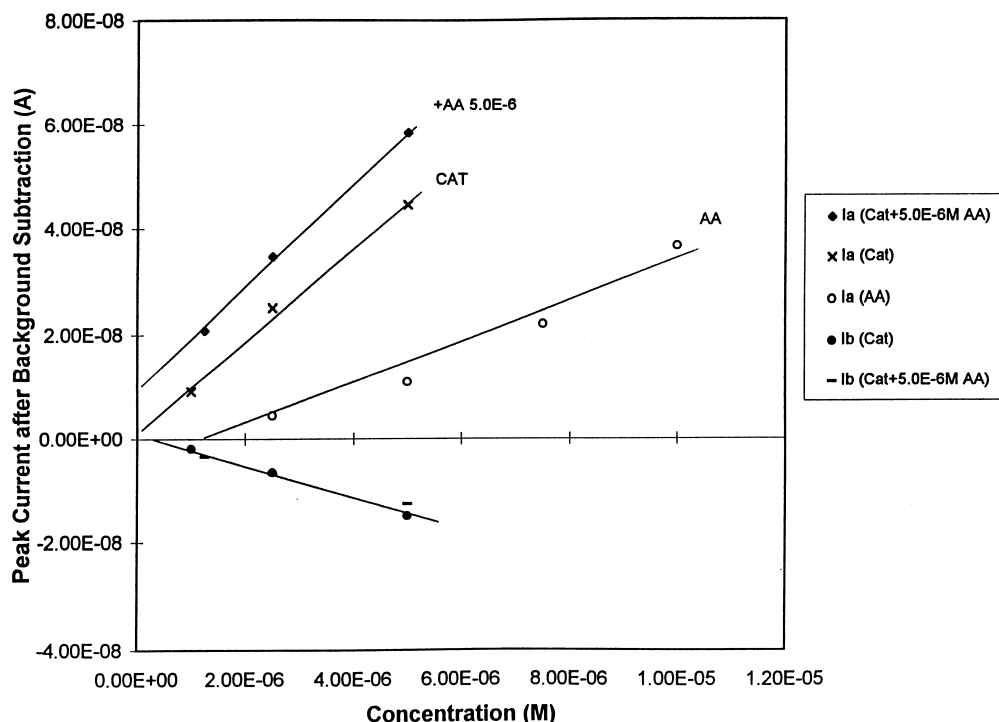


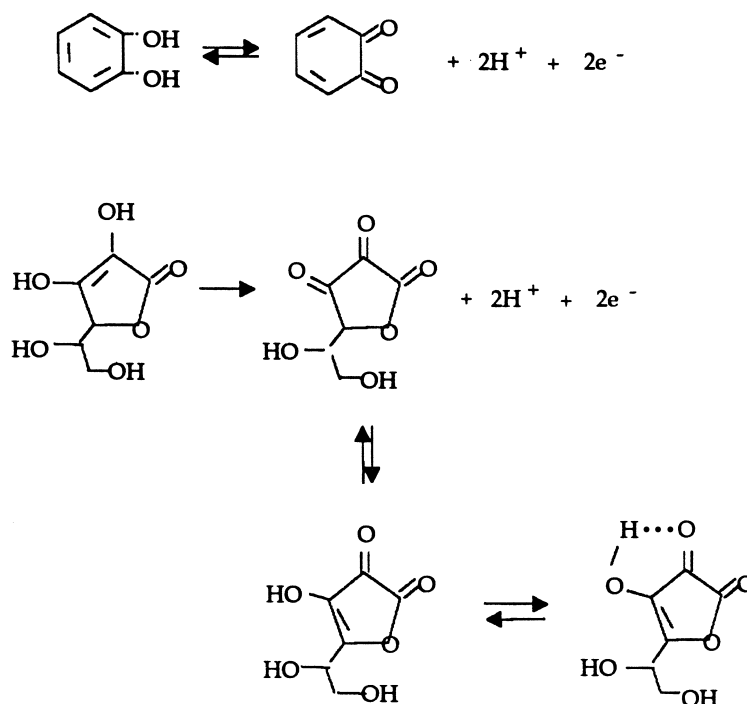
Fig. 8. Calibration curves for determination of catechol in the presence of  $5.0 \times 10^{-6}$  M ascorbic acid using series dual-band P3MT/Pt electrode flow-injection amperometry at pH 7.4. Experimental conditions as in Fig. 5.

rent of the oxidized catechol to the oxidation current of pure catechol, measured from the reduction and oxidation calibration lines. The average collection efficiency is 0.31 for this dual-band P3MT/Pt electrode.

However, for the higher concentration solutions of catechol, ranging from  $1.0 \times 10^{-5}$  to  $5.0 \times 10^{-4}$  M, in the presence of different concentrations of ascorbic acid, suppression of the reduction current signals for the oxidized catechol was clearly observed at the downstream electrode of dual-band Pt, Au, glassy carbon, and P3MT electrodes at pH 7.4 when the concentration of ascorbic acid was greater than  $2.5 \times 10^{-5}$  M ascorbic acid. For example, the negative deviation is shown in Fig. 9, where a series dual-band glassy carbon electrode was used as the detector for flow-injection analysis. Potentials of the upstream A and downstream B electrodes were held at 0.6 and  $-0.1$  V, respectively, to achieve the limiting currents. The reduction calibration line of the oxidized catechol in the presence of  $5.0 \times 10^{-5}$  M of ascorbic acid deviates negatively from the reduction calibration line obtained from catechol alone and reduction calibration lines obtained from the catechol solutions in the presence of  $5.0 \times 10^{-6}$  and  $2.5 \times 10^{-5}$  M ascorbic acid, which are superimposed on that one obtained from catechol alone. On the other hand, the oxidation calibration lines for catechol in the pre-

sence of the different amount of ascorbic acid in this study are not parallel to that measured from catechol alone. Furthermore, some of the plots are not linear, when the concentration of ascorbic acid is high. Signal suppression and enhancement of the catechol oxidation in the presence of ascorbic acid are observed at the different electrode materials and at different concentrations. For example, the oxidation calibration curve of catechol in the presence of  $5.0 \times 10^{-5}$  M ascorbic acid in Fig. 9 shows signal enhancement at the higher catechol concentrations ( $2.5 \times 10^{-5}$  and  $5.0 \times 10^{-5}$  M) and signal suppression at the lower catechol concentration ( $1.0 \times 10^{-6}$  M). Signal enhancement and suppression result in a nonlinear behavior for the oxidation of catechol in the presence of ascorbic acid. Therefore, a synergistic effect is observed in the electrochemical detection of catechol in the presence of ascorbic acid. The enhancement of current signal of catechol oxidation in the presence of ascorbic acid was first reported by Wightman and coworkers [33]. They suggested that the dopamine oxidation in the presence of ascorbic acid at carbon electrodes resulted in a homogeneous catalytic oxidation of ascorbic acid, which caused an enhanced current signal. The signal suppression, on the other hand, could be explained by the interactions between catechol and ascorbic acid, and between their oxidized products.

Electrochemical reaction schemes for catechol and ascorbic acid are as follows:



Ascorbic acid and oxidized ascorbic acid are weak acids with  $\text{p}K_{\text{a}}$  of 4.17 and 3.90, respectively [40], and therefore, their anion forms predominate at pH 7.4. The anion form of ascorbic acid can bond to polar catechol and the anion form of oxidized ascorbic acid can bond to polar oxidized catechol by forming an intermolecular H-bond and charge-dipole interaction in the more concentrated solutions. These interactions could reduce their diffusion rates to the electrodes, or affect electrokinetic parameters, or a combination of both, which causes the signal suppression. This signal suppression is removed at pH 1.6, which is an indirect evidence of H-bonding and charge-dipole interaction as discussed in the following paragraph. In dilute solutions of catechol and ascorbic acid mixtures much less H-bonding and charge-dipole interaction will occur. Therefore, the analyte exhibits ideal behavior in such solutions and no deviations from the standard calibration lines are observed at pH 7.4.

If the H-bond formation and charge-dipole interaction between catechol and ascorbic acid, and between their oxidized products cause the signal suppression, it is necessary to break up these interactions for the quantitation of catechol and ascorbic acid. When similar dual-band electrode flow-injection amperometric detection is carried using glassy carbon and P3MT/glassy carbon at pH 1.6, ascorbic acid and the oxidized ascorbic acid are predominantly in their neutral forms. Therefore, the

charge-dipole interaction due to their anion forms is eliminated and hydrogen bonding is broken by an excess of hydrogen ions. The experimental results show that reduction calibration lines of the oxidized catechol in the presence of ascorbic acid at both dual-band glassy carbon and P3MT/glassy carbon electrodes are superimposed on that of catechol alone (Figs 10 and 11). There is no negative deviation even when the concentration of ascorbic acid is as high as  $10^{-4}$  M. Therefore, as described previously, the amount of catechol in the mixture can be determined based on the reduction calibration line of the pure oxidized catechol at the downstream electrode. However, when the concentration of catechol in the presence of  $5.0 \times 10^{-6}$  ascorbic acid is greater than  $2.0 \times 10^{-4}$  M, there is still a current suppression for the reduction of oxidized catechol. Also the signal enhancement still occurs for the oxidation calibration lines of catechol in the presence of ascorbic acid.

#### Collection efficiency of catechol using dual-band electrode flow-injection amperometry

Factors that might influence the collection efficiency for catechol using dual-band electrode flow-injection amperometry are the electrode material, electrode surface area, interelectrode spacing, flow rate, and pH value of the mobile phase. After the minimization of the negative deviation in the reduction of oxidized catechol in the presence of

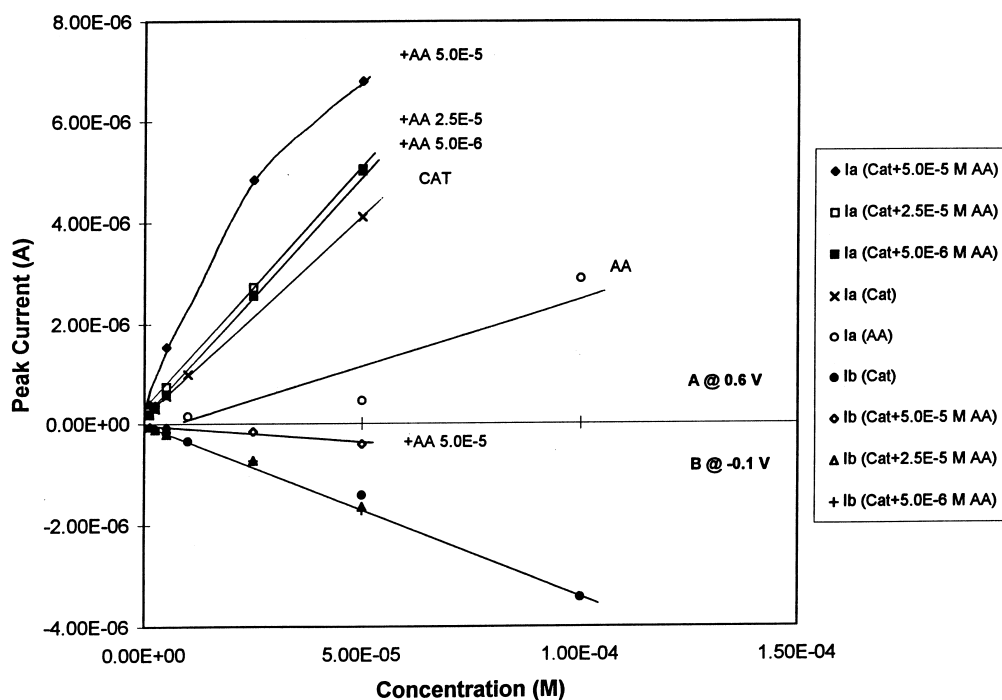


Fig. 9. Calibration curves for determination of catechol in the presence of ascorbic acid ranging from  $5.0 \times 10^{-6}$  to  $5.0 \times 10^{-4}$  M using series dual-band glassy carbon electrode flow-injection amperometry at pH 7.4 (interelectrode gap  $150 \mu\text{m}$ , band size  $5.5 \times 1.0 \text{ mm}$ ). Sensitivity  $11 \mu\text{A}$ . Other experimental conditions as in Fig. 5.

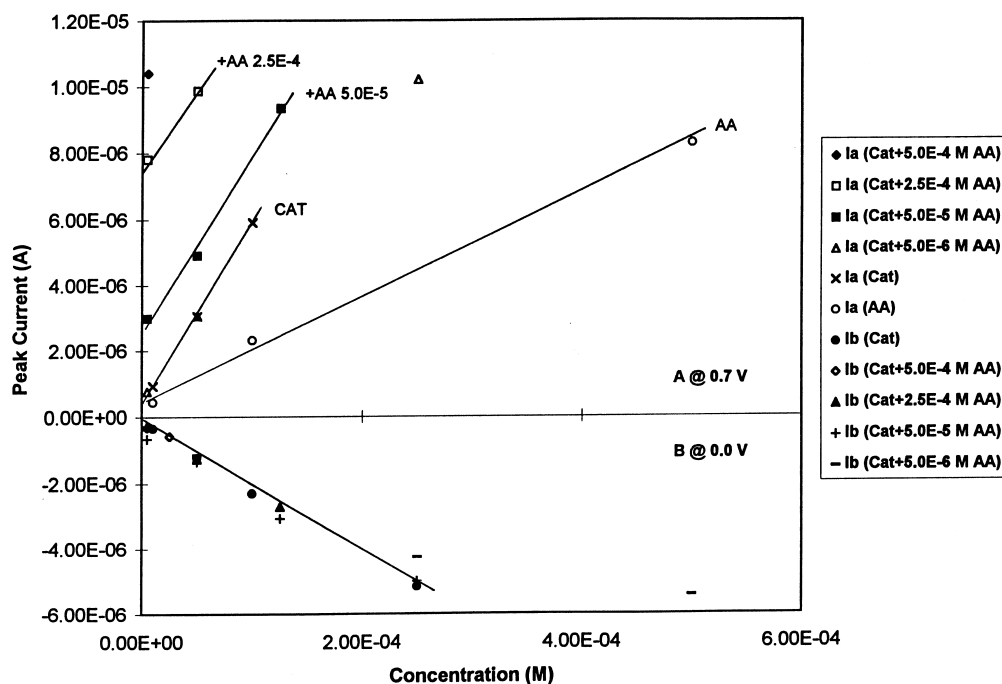


Fig. 10. Calibration curves for determination of catechol in the presence of ascorbic acid ranging from  $5.0 \times 10^{-5}$  to  $5.0 \times 10^{-4}$  M using series dual-band glassy carbon electrode flow-injection amperometry at pH 1.6 (interelectrode gap  $150 \mu\text{m}$ , band size  $5.5 \times 1.0 \text{ mm}$ ). Potentials of upstream A and downstream B electrode were held at 0.7 and 0.0 V, respectively. Flow rate  $1.0 \text{ ml/min}$ ; sensitivity  $11 \mu\text{A}$ ; mobile phase  $0.01 \text{ M H}_2\text{SO}_4$ .

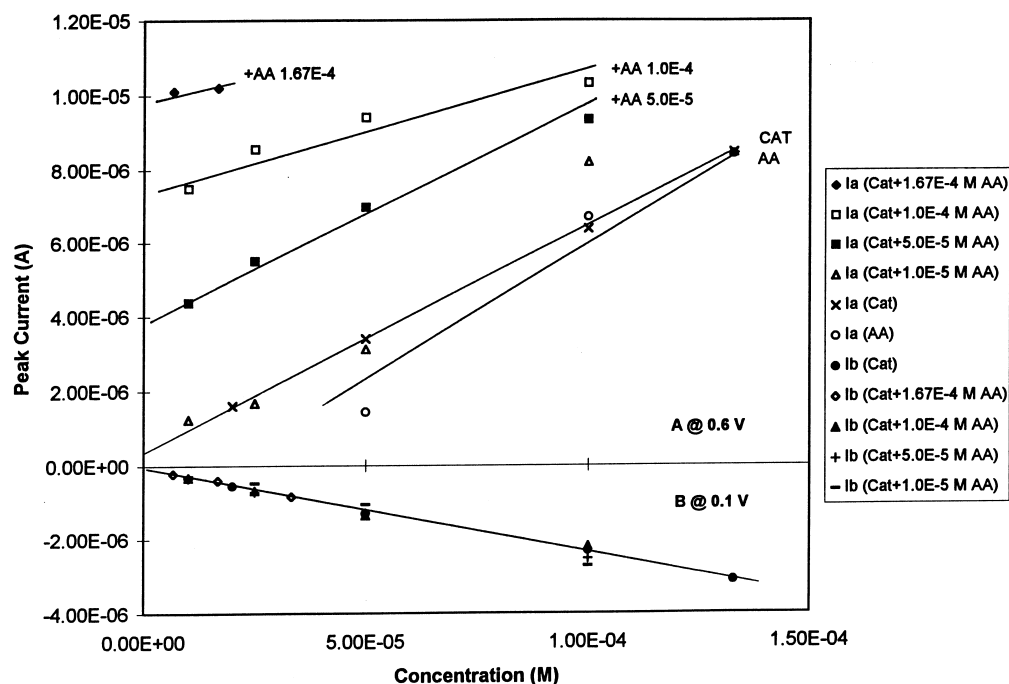


Fig. 11. Calibration curves for determination of catechol in the presence of ascorbic acid ranging from  $5.0 \times 10^{-5}$  to  $1.7 \times 10^{-4}$  M using series dual-band P3MT/glassy carbon electrode flow-injection amperometry at pH 1.6 (interelectrode gap  $150 \mu\text{m}$ , band size  $5.5 \times 1.0 \text{ mm}$ ). Potentials of upstream A and downstream B electrode were held at 0.6 and 0.0 V, respectively. Other experimental conditions as in Fig. 10.

ascorbic acid by lowering the pH value or using dilute solutions, the average collection efficiency for catechol in the presence of ascorbic acid is consistent with that of catechol alone. The collection efficiencies for catechol at dual-band Pt, Au, and glassy carbon electrodes at the flow rate of 1.0 ml/min are given in Table 1. With an interelectrode spacing around  $100 \mu\text{m}$ , collection efficiencies are 0.17, 0.24, and 0.39 for the different electrode materials, respectively. The glassy carbon electrode has the best collection efficiency among bare electrodes because of less fouling on its surface [2]. The collection efficiency results are comparable to those found for other systems. Previous studies by other groups reported that collection efficiencies at dual-disc glassy carbon electrodes were 0.35 for 4-methylcatechol and 3,4-dihydroxycinnamic acid [25], and 0.31 for norepinephrine, dopamine, and 3,4-dihydroxyphenylacetic acid [22]. At ring-disk car-

Table 1. Collection efficiency (CE) of catechol at series dual-band Pt, Au and glassy carbon electrodes\*

	Electrode and solution pH			
	Pt	Au	Glassy carbon	
	pH 7.4	pH 7.4	pH 1.6	pH 7.4
CE	0.17	0.24	0.36	0.42

\*Interelectrode gaps for dual-band Pt, Au and glassy carbon electrodes are 150, 95 and  $150 \mu\text{m}$ .

bon microelectrodes the collection efficiency for catecholamines ranged from 0.25 to 0.35 [27]. The collection efficiency for catechol at dual-band P3MT electrodes formed on Pt and glassy carbon substrates is about 0.31 (Table 2). Band sizes ranging from  $0.25 \text{ mm}^2$  for P3MT/Pt and P3MT/Au electrodes to  $5.5 \text{ mm}^2$  for P3MT/glassy carbon electrodes have no effect on the collection efficiency for catechol. This is consistent with Bard's observation that there is no discernible difference in collection efficiency as long as the area ratio of generator and collector is unity [37].

Interelectrode gaps ranging from 0.1 to 0.5 mm also produce no effect on the collection efficiency for catechol at P3MT electrodes (Table 2). The collection efficiency measured by the hydrodynamic

Table 2. Collection efficiency (CE) of catechol at series dual-band P3MT/Pt and P3MT/glassy carbon electrodes\*

	Electrode and solution pH				
	P3MT/Pt <sup>1</sup>	P3MT/Pt <sup>2</sup>	P3MT/GC <sup>1</sup>	P3MT/GC <sup>2</sup>	
	pH 7.4	pH 7.4	pH 1.6	pH 7.4	pH 7.4
CE	0.30	0.30	0.36	0.32	0.29

\*Interelectrode gaps for dual-band P3MT/Pt<sup>1</sup> and P3MT/Pt<sup>2</sup> electrodes are 80 and  $150 \mu\text{m}$ .

Interelectrode gaps for dual-band P3MT/GC<sup>1</sup> and P3MT/GC<sup>2</sup> electrodes are 150 and  $420 \mu\text{m}$ .

voltammograms does not change with the flow rate ranging from 0.5 to 3.0 ml/min (residence time in the electrochemical cell ranging from 1 to 0.16 s).

### CONCLUSIONS

Catechol ( $10^{-6}$ – $10^{-4}$  M) in the presence of ascorbic acid ( $10^{-6}$ – $10^{-4}$  M) can be determined by dual electrode flow-injection amperometry. Contents of catechol can be determined by the reduction calibration line of oxidized catechol at the downstream electrode, while contents of ascorbic acid can be determined by its oxidation calibration line at the upstream electrode after subtracting the catechol contribution. Negative deviations from the ideal calibration curves indicate the interactions between catechol and ascorbic acid, and between their oxidized products in the more concentrated solutions ( $>10^{-5}$  M) and at the physiological pH 7.4. These deviations can be minimized by lowering the solution pH value to 1.6. H-bonding and charge–dipole interactions are proposed to explain the negative deviations. Interelectrode gaps ranging from 0.1 to 0.5 mm between dual-band electrodes and flow rates varying from 0.5 to 3.0 ml/min have no effect on the collection efficiency for catechol. Dual-band P3MT as well as dual-band glassy carbon electrodes have the best collection efficiency for catechol.

### ACKNOWLEDGEMENTS

The technical assistance of Richard Shaw at the Surface Science Center and the L-S-T fellowship from Department of Chemistry, University of Cincinnati, are gratefully acknowledged.

### REFERENCES

1. R. N. Adams, *Anal. Chem.* **48**, 1126A (1976).
2. R. D. O'Neill, *Analyst* **119**, 767 (1994).
3. G. Nagy, M. E. Rice and R. N. Adams, *Life Sci.* **31**, 2611 (1982).
4. G. A. Gerhardt, A. F. Oke, G. Nagy, B. Moghaddam and R. N. Adams, *Brain Res.* **290**, 390 (1984).
5. K. J. Renner, L. Pazos and R. N. Adams, *Brain Res.* **577**, 49 (1992).
6. C. D. Blaha and R. F. Lane, *Brain Res. Bull.* **10**, 861 (1983).
7. R. A. Saraceno, J. G. Pack and A. G. Ewing, *J. Electroanal. Chem.* **197**, 265 (1986).
8. H. B. Mark Jr., N. Atta, Y. L. Ma, K. L. Petticrew, H. Zimmer, Y. Shi, S. K. Lunsford, J. F. Rubinson and A. Galal, *Bioelectrochem. Bioener.* **38**, 229 (1995).
9. R. M. Wightman, L. J. May and A. C. Michael, *Anal. Chem.* **60**, 769A (1988).
10. R. F. Lane, A. T. Hubbard, K. Fukunaga and R. J. Blanchard, *Brain Res.* **114**, 346 (1976).
11. J. Millar, J. A. Stamford, Z. L. Kruk and R. M. Wightman, *Eur. J. Pharmacol.* **109**, 341 (1985).
12. L. B. Anderson and C. N. Reilley, *J. Electroanal. Chem.* **10**, 295 (1965).
13. D. T. Napp, D. C. Johnson and S. Bruckenstein, *Anal. Chem.* **39**, 481 (1967).
14. D. A. Roston, R. E. Shoup and P. T. Kissinger, *Anal. Chem.* **54**, 1417A (1982).
15. C. L. Blank, *J. Chromatogr.* **117**, 35 (1976).
16. G. W. Schieffer, *Anal. Chem.* **52**, 1994 (1980).
17. L. A. Allison and R. E. Shoup, *Anal. Chem.* **55**, 8 (1983).
18. S. M. Lunte, *J. Chromatogr.* **384**, 371 (1981).
19. D. Madigan, I. McMurrugh and M. R. Smyth, *Analyst* **119**, 863 (1994).
20. R. J. Fenn, S. Siggia and D. J. Curran, *Anal. Chem.* **50**, 1067 (1978).
21. M. Goto, T. Nakamura and D. Ishii, *J. Chromatogr.* **226**, 33 (1981).
22. G. S. Mayer and R. E. Shoup, *J. Chromatogr.* **255**, 533 (1983).
23. C. E. Lunte and P. T. Kissinger, *Anal. Chem.* **55**, 1458 (1983).
24. W. A. MacCrehan and R. A. Durst, *Anal. Chem.* **53**, 1700 (1981).
25. D. A. Roston and P. T. Kissinger, *Anal. Chem.* **54**, 429 (1982).
26. D. M. Radzik, J. S. Brodbelt and P. T. Kissinger, *Anal. Chem.* **56**, 2927 (1984).
27. M. Zhong, J. Zhou, S. M. Lunte, G. Zhao, D. M. Giolando and J. R. Kirchhoff, *Anal. Chem.* **68**, 203 (1996).
28. P. T. Kissinger, C. R. Preddy, R. E. Shoup and W. R. Heineman, in *Laboratory Techniques in Electroanalytical Chemistry*, 2nd edn, ed. W. R. Heineman and P. T. Kissinger. Marcel Dekker, 1996.
29. A-1302 Electrode Polishing and Care. Bioanalytical Systems, West Lafayette, IN, 1995.
30. H. Zhang, S. K. Lunsford, I. Marawi, J. F. Rubinson and H. B. Mark Jr., *J. Electroanal. Chem.* **424**, 101 (1997).
31. E. A. Blubaugh, G. Russell, M. Racke, D. Blubaugh, T. H. Ridgway and H. B. Mark Jr., in *Diagnostic Biosensor Polymers*, ed. A. M. Usmani and N. Akmal. Symposium Series ACS Publications, 1994, pp. 137.
32. N. F. Atta, I. Marawi, K. L. Petticrew, H. Zimmer, H. B. Mark Jr. and A. Galal J., *J. Electroanal. Chem.* **408**, 47 (1996).
33. M. A. Dayton, A. G. Ewing and R. M. Wightman, *Anal. Chem.* **52**, 2392 (1980).
34. G. Gerhardt and R. N. Adams, *Anal. Chem.* **54**, 2618 (1982).
35. D. Robinson, J. E. Anderson and J. Lin, *J. Phys. Chem.* **94**, 1003 (1990).
36. W. Peng, B. J. Seddon, X. Zhou and Z. Zhao, *Fenxi Huaxue* **20**, 495 (1992).
37. A. J. Bard, J. A. Crayston, G. P. Kittlesen, T. V. Shea and M. S. Wrighton, *Anal. Chem.* **58**, 2321 (1986).
38. G. Zhao, D. M. Giolando and J. R. Kirchhoff, *Anal. Chem.* **67**, 1491 (1995).
39. Z. Fang, *Flow Injection Separation and Preconcentration*. VCH, Weinheim, Germany, 1993.
40. The Merck Index, 12th edn, ed. S. Budavari *et al.* Merck and Co., Whitehouse Station, NJ, 1996.